Journal of
Applied Crystallography
ISSN 0021-8898

Received 19 October 2012
Accepted 25 November 2012

Polarized neutron Laue diffraction on a crystal containing dynamically polarized proton spins

F. M. Piegsa,[a,b]* M. Karlsson,[c,d]* B. van den Brandt,[e] C. J. Carlile,[c] E. M. Forgan,[f] P. Hautle,[e] J. A. Konter,[e] G. J. McIntyre[a,g] and O. Zimmer[a]

[a]Institut Laue–Langevin, BP 156, F-38042 Grenoble, France, [b]Institute for Particle Physics, ETH Zürich, CH-8093 Zürich, Switzerland, [c]European Spallation Source ESS AB, PO Box 176, SE-221 00, Lund, Sweden, [d]Department of Applied Physics, Chalmers University of Technology, SE-41296 Göteborg, Sweden, [e]Paul Scherrer Institute, CH-5232 Villigen PSI, Switzerland, [f]School of Physics and Astronomy, University of Birmingham, Birmingham B15 2TT, UK, and [g]Australian Nuclear Science and Technology Organisation, Locked Bag 2001, Kirrawee DC NSW 2232, Australia. Correspondence e-mail: florian.piegsa@phys.ethz.ch, maths.karlsson@chalmers.se

A polarized neutron Laue diffraction experiment on a single crystal of neodymium-doped lanthanum magnesium nitrate hydrate containing polarized proton spins is reported. By using dynamic nuclear polarization to polarize the proton spins, it is demonstrated that the intensities of the Bragg peaks can be enhanced or diminished significantly, whilst the incoherent background, due to proton spin disorder, is reduced. It follows that the method offers unique possibilities to tune continuously the contrast of the Bragg reflections and thereby represents a new tool for increasing substantially the signal-to-noise ratio in neutron diffraction patterns of hydrogenous matter.

1. Introduction

Hydrogen atoms play a key role in many materials and biological systems of high interest; examples are biomolecules, fuel cells and soft condensed matter. Neutron diffraction studies of such hydrogenous matter generally suffer from a strong featureless background due to incoherent scattering by the protons. The incoherent scattering arises because the proton spins are normally completely disordered, and the scattering length – the strength of the neutron–proton interaction – depends strongly on the relative orientation of proton and neutron spins. A common way to reduce this incoherent scattering is to replace the hydrogen by deuterium, since the incoherent scattering length of deuterium is far smaller than that of hydrogen. However, producing such samples is difficult, expensive and, for some materials (*e.g.* complex biomolecules), often impossible. Equally well, isostructuralism cannot be guaranteed. Another method to reduce, or even remove completely, the incoherent scattering by the hydrogen atoms is to align the spins of the neutrons and protons so that they are parallel (Stuhrmann, 2004; Stuhrmann & Nierhaus, 1996; Zhao, 2005; van den Brandt *et al.*, 2007, 2006). This is seen from Fig. 1, which shows the polarization-dependent coherent and incoherent cross sections for hydrogen, according to

$$\sigma_{\rm coh} = 4\pi\left[b_{\rm c}^2 + 2\left(\tfrac{1}{3}\right)^{1/2} P_{\rm n} P_{\rm I} b_{\rm c} b_{\rm i} + \tfrac{1}{3} P_{\rm I}^2 b_{\rm i}^2\right] \quad (1)$$

and

$$\sigma_{\rm inc} = 4\pi b_{\rm i}^2\left(1 - \tfrac{2}{3} P_{\rm n} P_{\rm I} - \tfrac{1}{3} P_{\rm I}^2\right), \quad (2)$$

where $P_{\rm I}$ and $P_{\rm n}$ are the polarizations of the protons and the incident neutron beam, respectively, $b_{\rm c}$ is the coherent scattering length of hydrogen, and $b_{\rm i}$ is the incoherent scattering length (Stuhrmann, 2004; Dianoux & Lander, 2003). When the spins of the neutrons and the protons are parallel ($P_{\rm n}P_{\rm I} = 1$) there is no incoherent scattering, and when they are antiparallel ($P_{\rm n}P_{\rm I} = -1$) the incoherent scattering is maximized. It is also evident from Fig. 1 that the coherent scattering cross section increases from 1.8 to 14.7 barns (1 barn = 10^{-28} m^{-2}) when the spins are aligned, and hence a huge improvement in the signal-to-noise ratio will be observed. The latter effect was originally demonstrated in the 1970s for a monochromatic neutron beam and a single crystal of neodymium-doped

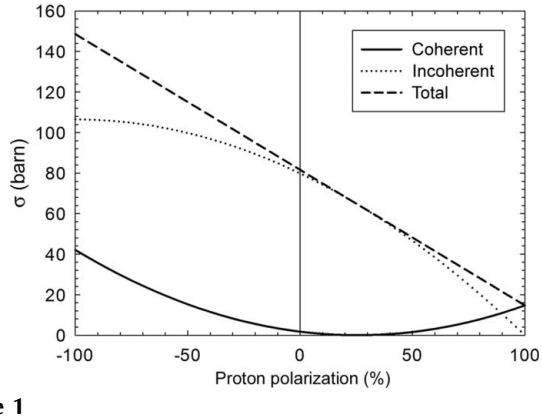

Figure 1
Coherent, incoherent and total scattering cross section of hydrogen as a function of the proton polarization for fully polarized neutrons, *i.e.* $P_{\rm n} = 1$.

lanthanum magnesium nitrate hydrate, $La_2Mg_3(NO_3)_{12}\cdot 24H_2O$ (LMN:Nd) (Hayter *et al.*, 1974). Here, we report on a polarized neutron Laue diffraction experiment (Wollan *et al.*, 1948) on a single crystal of LMN:Nd containing polarized protons, with the goal to demonstrate experimentally that a significant improvement of the signal-to-noise ratio of the Laue patterns can be achieved. The measurements were performed at the FUNSPIN beamline at the continuous spallation neutron source SINQ at the Paul Scherrer Institute (PSI), Switzerland (Zejma *et al.*, 2005).

2. Experimental setup

A key aspect of the experiment described here is the method to achieve a sizable nuclear spin polarization of the protons in the single-crystal sample. The brute force approach, *i.e.* cooling a sample that is situated in a strong magnetic field to temperatures in the millikelvin range, will not lead to the desired result of a high nuclear polarization because of the excessively long nuclear spin relaxation times under these conditions (van den Brandt *et al.*, 2000). On the other hand, the so-called dynamic nuclear polarization (DNP) technique allows the polarization of nuclear spins in a solid under less restrictive conditions (Abragam & Goldman, 1978, 1982; Wenckebach, 2008).

As a prerequisite for DNP the sample needs to contain a certain number of unpaired electrons (paramagnetic centres): typically 0.1% of the nuclear concentration. As the electron spins possess a much larger magnetic moment than the nuclear spins and a considerably shorter spin-lattice relaxation time compared to the nuclear spins, they easily reach polarizations of almost 100% at moderate temperatures of 1 K and magnetic fields of 2.5 T. This electron spin ordering can be transferred to the nuclear spins by irradiation of microwaves close to the electron paramagnetic resonance frequency, because of the dipolar interaction between the nuclear and electron spins. LMN:Nd with its high content of hydrogen (proton density: 3.9×10^{22} cm^{-3}) is a well known crystal to be polarized by means of the effect of DNP (Schmugge & Jeffries, 1962, 1965; Atkinson, 1966; Leslie *et al.*, 1980; Anderson *et al.*, 1977) and hence represents a good candidate material to perform a proof-of-principle experiment.

A schematic drawing of the polarized neutron Laue setup is presented in Fig. 2 (right). The incoming white cold neutron beam (polarization $P_n \geq 95\%$) is collimated horizontally and vertically using an arrangement of two Soller collimators (Piegsa, 2009) and several diaphragms, resulting in a circular beam with a diameter of 5 mm, a divergence of approximately 2 mrad (FWHM) and the spectral distribution presented in Fig. 2 (left). The neutron flux at the sample position is about 2.5×10^5 cm^{-2} s^{-1} at a proton current of 1.5 mA on the SINQ spallation target. The LMN:Nd crystal with a cross section of 10×10 mm and a thickness of 5 mm was placed inside a multi-mode microwave cavity which was top loaded into a dedicated ^{4}He evaporation DNP cryostat, with a base temperature of 1.05 K and a vertical split-pair 2.5 T magnet (with a heat load of 50 mW a temperature of 1.10 K is reached).

The concept of this type of cryostat for the polarization of nuclear spins goes back to the 1960s (Roubeau, 1976). The characteristics of this design are firstly that the system consists of a cryostat and an insert tightly fitting into the cryostat. The sample is mounted onto the insert. In its final position the insert is fully contained in its own pumping tube and can be taken out or re-inserted within a short time even into the cold cryostat (thus allowing loading of samples kept at 77 K). Secondly, the thin tube around the region of the insert where the sample is mounted is directly in the isolation vacuum of the cryostat, thus minimizing the amount of material in the beam path. In this experiment the tube thickness was 0.25 mm of $AlMg_3$. The beam also has to pass through the outer vacuum window (0.2 mm of pure aluminium) and the aluminium radiation shields (2×10 µm). These thicknesses are on the incoming path; the outgoing path is equivalent. This careful choice of material reduces the background from neutrons scattered out of the incident and transmitted beams. A further development at PSI incorporated a removable central access (van den Brandt *et al.*, 1990), enabling a faster sample change, or an angle-reproducible loading of special-shaped samples, or even the use of multi-stage or dummy-

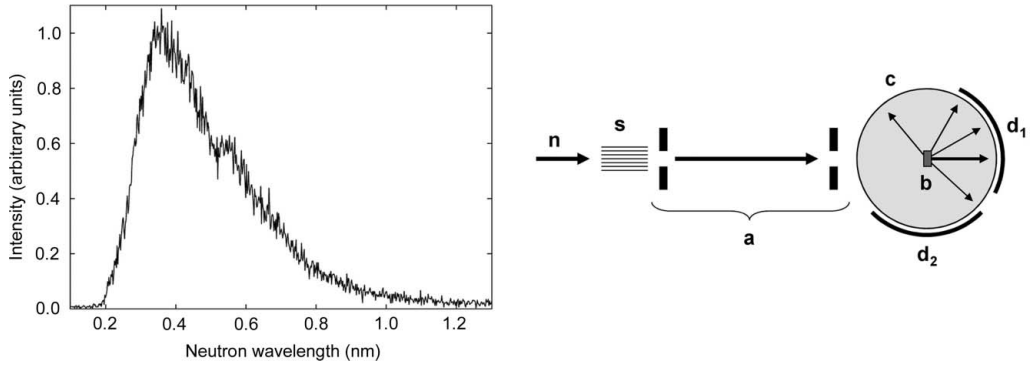

Figure 2
Left: spectrum of the polarized neutron beam with a peak flux at approximately 0.36 nm. This spectrum was determined by a separate time-of-flight measurement. Right: schematic top view of the polarized Laue setup. The incident neutron beam (n) is collimated by two Soller-type collimators (s) and several diaphragms (a). The neutrons are scattered by the LMN:Nd crystal (b) situated in the DNP cryostat (c). The scattering pattern is recorded using standard neutron image plates (d_1 and d_2) which surround the cryostat.

samples for background measurements. The last feature was also used in this experiment. Detailed schematic drawings of the cryostat and the insert are shown in Fig. 3.

Additionally, small permanent magnets were installed within the split-pair magnet, creating a weak horizontal holding field to avoid depolarization of the neutron beam as it passes through the zero-field region of the superconducting magnet. This horizontal field does not influence the homogeneity of the main magnetic field at the sample position, which is better than 2×10^{-4}. This homogeneity is necessary to establish a uniform polarization over the entire sample. Positive proton spin polarization was achieved by irradiating with microwaves with a frequency of 78.965 GHz at a magnetic field of 2.06 T into the sample cavity using a 10 W extended interaction oscillation tube (electron g factor in LMN:Nd: $g_{\perp} = 2.70$). The proton polarization was measured with continuous wave NMR using a so-called Q-meter which was calibrated by means of the thermal equilibrium polarization (Court *et al.*, 1993). In order to provide a constant nuclear polarization over a period of several hours, continuous irradiation with microwaves was indispensable, as the nuclear spin relaxation time at 2.06 T and 1.05 K was determined to be about 150 min.

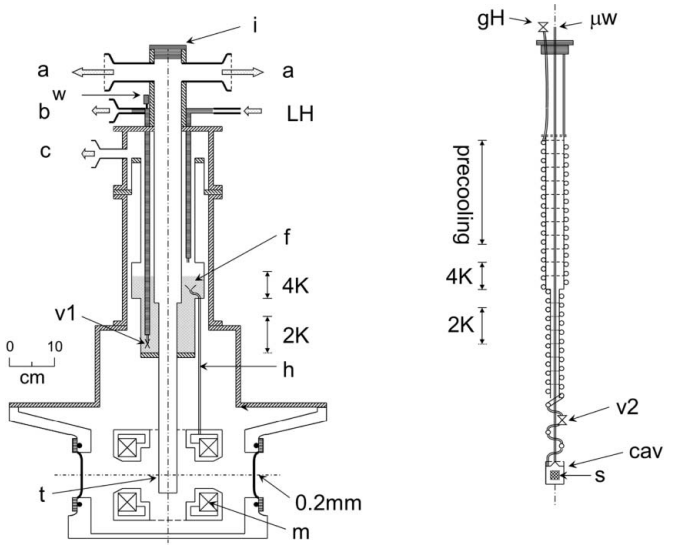

Figure 3
Left (cryostat): liquid helium (LH) enters the cryostat *via* a transfer line. The helium bath is drawn shaded and the level where the temperature is around 4 K corresponding to the vapour pressure of 1 bar of outlet (c) is indicated (arrows 4 K). In the lower region temperatures around the λ transition at 2.17 K are reached by pumping through a needle valve (v1), which is operated from the top with an actuator wheel (w). This region (arrows 2 K) is pumped off *via* (b) and the temperature gradient is established by the temperature-dependent density. The superconducting magnet (m), which produces a vertical field, is encapsulated in a metal housing and helium is introduced *via* a helium line (h). A funnel (f) is used during precooling of the magnet. The windows for the horizontal neutron beam are shown with thicknesses of 0.2 mm. Pumping ports (a) serve to pump the liquid helium bath around the sample in the case where it is mounted onto the insert and introduced *via* the top opening (i) into the tube (t). Right (insert): The sample (s) is mounted in the microwave cavity (cav) attached to the microwave guide, allowing microwaves (μw) to enter from the top. Gaseous helium (gH) enters through a valve, gets precooled, condenses and cools further in the indicated regions (heat exchanger) if placed in the cryostat with the corresponding temperature distribution. The thermal contact takes place *via* the evaporating helium gas that streams back and leaves the cryostat by pumping on ports (a) on the cryostat drawing. The flow of the liquid ^{4}He is regulated by means of a needle valve (v2).

3. Results and discussion

Laue patterns were recorded using two standard neutron-sensitive image plates with a size of 400 × 200 mm, covering a total horizontal angle of about 210° and a vertical angle of ±12° (owing to absorption of the scattered neutrons in the coils of the magnet only about half of the vertical dimension of the image plate could be used). The image plates were read out with a spatial resolution of 200 μm using a Fujifilm BAS-2500 scanner and the patterns obtained were normalized to the total neutron flux by means of a neutron monitor detector placed in the white beam.

In order to observe the effect on the neutron Laue pattern intensity and the incoherent background, we performed

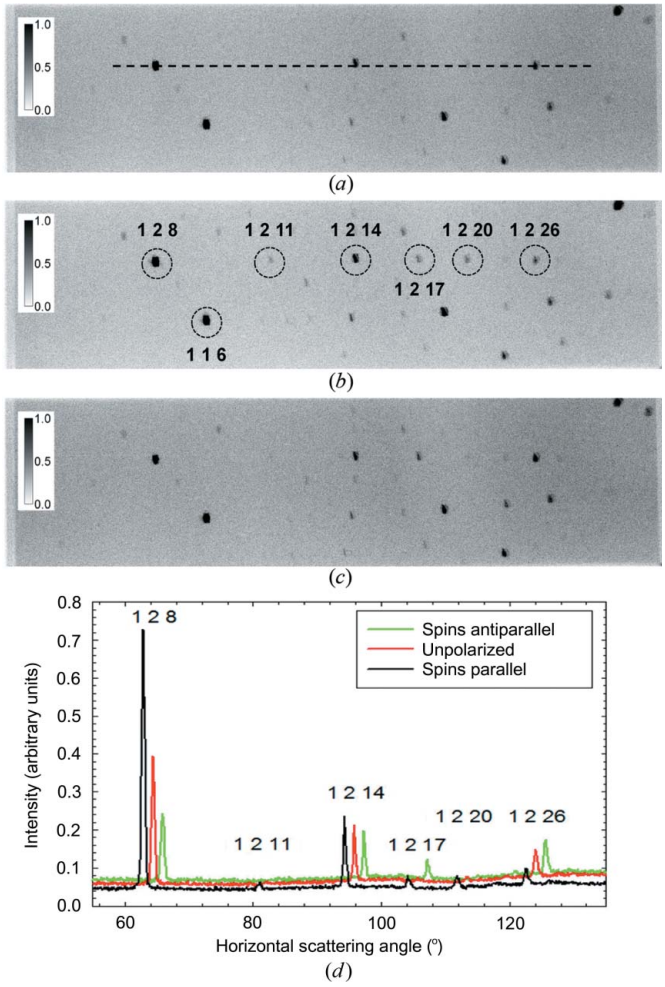

Figure 4
Normalized and background-subtracted Laue patterns of image plate d_2: (*a*) unpolarized sample, (*b*) proton and neutron spins parallel, and (*c*) spins antiparallel (proton polarization in both cases is approximately 35%). (*d*) Cuts through all three patterns along the dashed horizontal line indicated in (*a*). For clarity the plots for parallel and antiparallel spins have been shifted by −1.5 and +1.5° in horizontal scattering angle, respectively.

Table 1
Intensities and intensity ratios for a selection of Laue reflections obtained from the data presented in Fig. 4 for the unpolarized sample ($I_{\uparrow-}$), and for samples polarized parallel ($I_{\uparrow\uparrow}$) and antiparallel ($I_{\uparrow\downarrow}$) with respect to the neutron spin.

hkl	Multiplicity	λ (nm)	$I_{\uparrow-}$	$I_{\uparrow\uparrow}$	$I_{\uparrow\downarrow}$	$I_{\uparrow\uparrow}/I_{\uparrow-}$	$I_{\uparrow\downarrow}/I_{\uparrow-}$	$I_{\uparrow\uparrow}/I_{\uparrow\downarrow}$
116	3	0.4986	114290 (512)	136192 (520)	76128 (448)	1.19	0.67	1.79
128	1	0.3154	102135 (488)	2040 (616)	41663 (368)	2.00	0.41	4.90
1 2 11	1	0.3281	108 (288)	4513 (272)	756 (248)	41.8	7.00	5.97
1 2 14	1	0.3144	35023 (376)	48455 (384)	25683 (328)	1.38	0.73	1.89
1 2 17	1	0.2920	974 (296)	9020 (296)	10473 (304)	9.26	10.8	0.86
1 2 20	1	0.2682	3266 (304)	8597 (304)	1299 (280)	2.63	0.40	6.62
1 2 26	1	0.2257	21228 (360)	12141 (320)	22882 (352)	0.57	1.08	0.53

measurements with an unpolarized sample and with a sample with a proton polarization of 30–35%. The polarization of the incoming neutron beam could be flipped by means of an adiabatic spin flipper, such that the spins of the protons and neutrons could be oriented either parallel or antiparallel. The results for these three cases are depicted in Fig. 4. Each image shows the Laue pattern for the horizontal scattering angle from 41° to about 146°, which corresponds to image plate d_2 in Fig. 2 (right). The exposure time for each pattern was about 10 h. The instrumental background, *i.e.* the background from sources other than the incoherent scattering of the sample, is obtained in the same manner, but without the sample in the cryostat. This background contributes approximately 35% to the total background in the case of the unpolarized sample and is subtracted from each of the three patterns.

The relative change of the incoherent scattering due to the proton polarization can be determined by averaging the neutron intensity over several areas of the pattern where there are no Laue reflections. In the case where the neutron and the proton spins are aligned parallel the incoherent scattering reduces to 76 (2)%, while it increases to 115 (2)% for antiparallel spins. These results are in good agreement with the calculated values of 73–77% and 117–119%, if one assumes that the incoherent scattering is solely caused by the protons in the sample and a polarization of 30–35%.

The Laue reflections were indexed using the program *LAUEGEN* (Campbell *et al.*, 1998; Campbell, 1995) and integrated using the program *ARGONNE-BOXES* (Wilkinson *et al.*, 1988), with the true counting statistics estimated from the observed point-by-point variations in the local background (Wilkinson *et al.*, 2009). The intensities for a selection of Laue reflections are summarized in Table 1. It is seen that the intensities of the individual reflections can be changed significantly by spin polarization. For example, in an unpolarized sample, the reflection 1 2 11 is practically undetectable, while it becomes clearly visible in the case of parallel spins. Significant changes in intensity with polarization are also observed in some reflections in the row 11*l*. Because the intensity of Bragg reflections may be thereby increased or decreased, an improvement of the signal-to-noise ratio is not observed for all the recorded reflections. However, we do note that, for large-unit-cell biological crystals, the intensity of incoherent background compared to that of the Laue reflections will be much greater than for our proof-of-principle experiment. Hence, the reduction of this background by polarization of the sample will be even more important in that case.

4. Conclusions

In conclusion, we have shown that the polarization of protons opens up the possibility to tune the contrast of the Bragg reflections, whilst the incoherent scattering is reduced, in a quite predictable manner. This concept of utilizing the strong spin dependence of the scattering cross sections of hydrogen may be very favourably employed to improve substantially the poor signal-to-noise ratio in neutron diffraction experiments on samples with a large hydrogen content. It follows that the technique may provide answers to specific questions on, for example, hydrogen positions or protonation states and hence may have a huge impact on a large range of disciplines, ranging from hard and soft condensed matter to pharmaceutical biology. For the widespread use of DNP in neutron Laue diffraction, the method is, however, accompanied by a few demanding challenges and open questions: (i) Which paramagnetic centres can be used and can they be implanted in a crystal, notably a biological crystal, of a sufficient size? (ii) What is the level of proton polarization that can be achieved? (iii) What is the gain compared to deuteration? (iv) How can the sample environment be optimized for Laue diffraction? Although the answering of these questions requires further exploration, we can here give tentative responses:

(i) DNP on biological macromolecules was originally performed by adding a small percentage of a bulky Cr^{5+} complex, $C_{12}H_{22}CrO_4Na\cdot H_2O$, to a solution containing the macromolecule of interest, which was then frozen to form a glassy sample (Stuhrmann, 2004; Willumeit *et al.*, 1996). The paramagnetic carrier would generally need to be considerably smaller than this complex to promote or maintain translational symmetry in the crystalline state. The smaller TEMPO free radical, recently also used to create hyperpolarized substances for biological MRI (Kurdzesau *et al.*, 2008), would be the first choice.

(ii) The polarization of 35% achieved in this experiment is particularly unsuitable for determination of hydrogen positions since it corresponds to a coherent cross section of hydrogen of nearly zero (Fig. 1). Achieving a polarization of at least 50% is desirable and seems possible with state-of-the-art DNP equipment. However, it might be necessary to reduce the sample temperature further and/or increase the magnetic field strength to improve the nuclear spin relaxation time, which constrains the maximum polarization. Much of the further development to increase the polarization can be done, however, without neutrons, using, for example, NMR to measure the polarization.

(iii) Where it is possible and does not change the structure or function, deuteration is at present still preferable to proton polarization, since a given percentage average deuteration can yield the same reduction in incoherent background as the

same percentage proton polarization. However, when deuteration is not possible or for structure determination, the polarization technique offers unique possibilities.

(iv) The intrinsically smaller sample sizes available and desirable for Laue diffraction reduce the requirements on the spatial extent of the field homogeneity and the gap between the magnet pole pieces, which should allow a scaling down of the apparatus and/or an enlargement of the solid angle of detection.

We gratefully acknowledge help by the neutron radiography group of PSI (C. Grünzweig, E. H. Lehmann and P. Vontobel), J. Kohlbrecher for fruitful discussions and P. Schurter for excellent technical support. Special microwave equipment was kindly provided to PSI by W. Th. Wenckebach. MK and CJC thank the Swedish Research Council for instrument development funding. The principal authors, FMP and MK, contributed equally to this work. This work was performed at the Swiss Spallation Neutron Source at the Paul Scherrer Institute, Villigen, Switzerland.

References

Abragam, A. & Goldman, M. (1978). *Rep. Prog. Phys.* **41**, 395–467.
Abragam, A. & Goldman, M. (1982). *Nuclear Magnetism: Order and Disorder.* Oxford University Press.
Anderson, M. R., Jenkin, G. T. & White, J. W. (1977). *Acta Cryst.* B**33**, 3933–3936.
Atkinson, H. H. (1966). *Proceedings of the International Conference on Polarized Targets and Ion Sources, Saclay*, p. 41. Paris: La Documentation Français.
Brandt, B. van den, Bunyatova, E. I., Hautle, P., Konter, J. A. & Mango, S. (2000). *Nucl. Instrum. Methods Phys. Res. Sect. A*, **446**, 592–599.
Brandt, B. van den, Glaettli, H., Grillo, I., Hautle, P., Jouve, H., Kohlbrecher, J., Konter, J. A., Leymarie, E., Mango, S., May, R. P., Michels, A., Stuhrmann, H. B. & Zimmer, O. (2006). *Eur. Phys. J. B*, **49**, 157–165.
Brandt, B. van den, Glättli, H., Hautle, P., Kohlbrecher, J., Konter, J. A., Michels, A., Stuhrmann, H. B. & Zimmer, O. (2007). *J. Appl. Cryst.* **40**, s106–s110.
Brandt, B. van den, Konter, J. A. & Mango, S. (1990). *Nucl. Instrum. Methods Phys. Res. Sect. A*, **289**, 526–531.
Campbell, J. W. (1995). *J. Appl. Cryst.* **28**, 228–236.
Campbell, J. W., Hao, Q., Harding, M. M., Nguti, N. D. & Wilkinson, C. (1998). *J. Appl. Cryst.* **31**, 496–502.
Court, G. R., Gifford, D. W., Harrison, P., Heyes, W. G. & Houlden, M. A. (1993). *Nucl. Instrum. Methods Phys. Res. Sect. A*, **324**, 433–440.
Dianoux, A.-J. & Lander, G. (2003). *ILL Neutron Data Booklet.* Philadelphia: OCP Science Imprint.
Hayter, J. B., Jenkins, G. T. & White, J. W. (1974). *Phys. Rev. Lett.* **33**, 696–699.
Kurdzesau, F., van den Brandt, B., Comment, A., Hautle, P., Janin, S., van der Klink, J. J. & Konter, J. A. (2008). *J. Phys. D Appl. Phys.* **41**, 155506.
Leslie, M., Jenkin, G. T., Hayter, J. B., White, J. W., Cox, S. & Warner, G. (1980). *Philos. Trans. R. Soc. London Ser. B*, **290**, 497–503.
Piegsa, F. M. (2009). *Nucl. Instrum. Methods Phys. Res. Sect. A*, **603**, 401–405.
Roubeau, P. (1976). *Proceedings of the 6th International Cryogenic Engineering Conference*, p. 99. Guildford: IPC Science and Technology Press.
Schmugge, T. J. & Jeffries, C. D. (1962). *Phys. Rev. Lett.* **9**, 268–270.
Schmugge, T. J. & Jeffries, C. D. (1965). *Phys. Rev.* **138**, 1785–1801.
Stuhrmann, H. B. (2004). *Rep. Prog. Phys.* **67**, 1073–1115.
Stuhrmann, H. B. & Nierhaus, K. H. (1996). *The Determination of the in situ Structure by Nuclear Spin Contrast Variation in Neutrons and Biology.* New York: Plenum Press.
Wenckebach, W. T. (2008). *Appl. Magn. Reson.* **34**, 227–235.
Wilkinson, C., Khamis, H. W., Stansfield, R. F. D. & McIntyre, G. J. (1988). *J. Appl. Cryst.* **21**, 471–478.
Wilkinson, C., Lehmann, M. S., Meilleur, F., Blakeley, M. P., Myles, D. A. A., Vogelmeier, S., Thoms, M., Walsh, M. & McIntyre, G. J. (2009). *J. Appl. Cryst.* **42**, 749–757.
Willumeit, R., Burkhardt, N., Diedrich, G., Zhao, J. K., Nierhaus, K. H. & Stuhrmann, H. B. (1996). *J. Mol. Struct.* **383**, 201–211.
Wollan, E. O., Shull, C. G. & Marney, M. C. (1948). *Phys. Rev.* **73**, 527–528.
Zejma, J. *et al.* (2005). *Nucl. Instrum. Methods Phys. Res. Sect. A*, **539**, 622–639.
Zhao, J. K. (2005). *Physica B*, **356**, 168–173.